coatings

MDPI

Article

Experimental Study of Atmospherically and Infrared-Dried Industrial Topcoats

Ivan Stojanović [1], Mirta Logar [1,*], Ivan Fatović [1], Vesna Alar [1] and Daniela Rakela-Ristevski [2]

[1] Chair of Materials Protection, Faculty of Mechanical Engineering and Naval Architecture, University of Zagreb, 10000 Zagreb, Croatia; ivan.stojanovic@fsb.hr (I.S.); ivan.fatovic@fsb.hr (I.F.); vesna.alar@fsb.hr (V.A.)
[2] Končar Steel Structures Inc., 10000 Zagreb, Croatia; daniela.rakela@koncar-mk.hr
* Correspondence: mirta.logar@fsb.hr

Abstract: In this paper, five different solvent-borne industrial topcoats were dried with infrared (IR) radiation and under atmospheric conditions. A comparison of physical, mechanical, chemical, and electrochemical properties of differently dried topcoats was made. The results of differential scanning calorimetry (DSC), Fourier-Transform Infrared Spectroscopy (FTIR), and adhesion of a topcoat to the metal substrate (determined by the pull-off test) indicate a higher degree of crosslinking of examined topcoats, which improves the coating's protective properties. Scratch hardness was determined by the pencil hardness test. Impact resistance was examined with a falling-weight test. Changes in the shade of the coating were examined by visual inspection and using a gloss meter. The electrochemical measurements of open circuit potential (OCP) and electrochemical impedance spectroscopy (EIS) were conducted. The thermal stability of topcoats was tested by thermogravimetric analysis (TGA). The results show overall better properties of IR-dried topcoats. In addition, topcoats dry significantly faster when IR radiation is applied, which makes this drying method very interesting for industrial application.

Keywords: industrial topcoats; polyurethane; polysiloxane; infrared drying; corrosion protection

check for updates

Citation: Stojanović, I.; Logar, M.; Fatović, I.; Alar, V.; Rakela-Ristevski, D. Experimental Study of Atmospherically and Infrared-Dried Industrial Topcoats. *Coatings* **2023**, *13*, 1343. https://doi.org/10.3390/coatings13081343

Academic Editor: Alexander Tolstoguzov

Received: 19 June 2023
Revised: 19 July 2023
Accepted: 27 July 2023
Published: 30 July 2023

Copyright: © 2023 by the authors. Licensee MDPI, Basel, Switzerland. This article is an open access article distributed under the terms and conditions of the Creative Commons Attribution (CC BY) license (https://creativecommons.org/licenses/by/4.0/).

1. Introduction

Metal corrosion is one of the biggest problems worldwide, especially in the industrial environment [1]. According to the National Association of Corrosion Engineers (NACE International) and data from 2013, the global cost of corrosion is estimated at USD 2.5 trillion, equivalent to 3.4% of the global GDP [2]. In order to slow down corrosion processes, it is important to wisely choose the material and to ensure good surface preparation, but also to use additional protection methods, such as coatings, cathodic protection, corrosion inhibitors, etc. [3,4]. The application of polymer coatings is one of the most commonly used corrosion protection methods. In this method, the metal substrate is usually coated with a coating system, which often consists of three layers: primer, intermediate coat, and topcoat. Organic coatings provide the best protection to the metal substrate if the barrier properties of the coating are good, that is, in the absence of defects (pores, scratches, etc.) that extend to the very surface of the protected metal, which can initiate corrosion [5,6].

Competitive pressure in the metal industry is increasing. To survive, it is necessary for the steel manufacturers to shorten the finishing time, which especially refers to the coating protection process, so that they can put as many products as possible on the market in the shortest possible time. One of the solutions for faster drying/curing of protective coatings is using radiation, such as infrared radiation (IR) [7]. Infrared drying enables fast evaporation of the solvent, but should be used with caution since too-fast evaporation can cause blistering [8]. In the process of radiation curing, a coating is crosslinked as a result of interacting with incident radiation, directly on a substrate [9]. Any industry that requires

drying, polymerization, or curing in manufacturing processes can use infrared radiation to speed up the process [10]. Currently, IR radiation is often used in the automotive industry to speed up the coating drying process, but more and more industries are turning to this solution [11]. For the industry, the simplest transition to this new technology is to apply IR radiation for drying coatings they already use. In order to enable a carefree transition to IR technology, it is necessary to conduct research on the IR-dried coatings' protective properties in comparison with the properties of conventionally dried coatings.

The curing or crosslinking of coatings is the formation of lateral connections of polymer chains. As a result of this process, the crosslinked polymer becomes harder, and its glass transition temperature shifts towards higher temperatures. Furthermore, mechanical strength and chemical resistance improve with a higher curing degree [12]. These properties reflect the degree of polymer crosslinking. However, making predictions about the coating curing process is a complex and expensive issue that requires a lot of experimental work in order to obtain a functional curing prediction model [10]. Because of that, experimental literature that describes this issue is rather scarce. Some researchers, like Saure et al. [13,14] and Geipel and Stephan [15], use FTIR to analyze the behavior of polymer coatings during drying. Others also use differential scanning calorimetry (DSC) and thermogravimetric analysis (TGA), like Vessot et al. [16] did, to study the drying and curing of polyurethane-based coatings. A fully cured coating should have good adhesion to the metal substrate and good corrosion resistance [17]. Many researchers, including Alsamuraee et al. [5], use electrochemical impedance spectroscopy (EIS) as a method to evaluate the state of the coating surface and its barrier properties, which are key to achieving the satisfactory corrosion resistance of the coating. Nevertheless, the impact of catalytic infrared radiation (CIR) on the top coating curing process and comparison to the conventional drying method by using comprehensive test methods have not been broadly explored.

The aim of this paper is to study the difference between atmospherically and infrared-dried/cured industrial topcoats. Liquid, solvent-borne industrial topcoats from two different manufacturers were examined. A comparison of physical, mechanical, corrosion, and chemical properties of differently dried topcoats was made. The adhesion of the topcoat to the metal substrate was tested using a pull-off adhesion test. The gloss of differently dried topcoats was compared using a gloss meter. The pencil hardness test was used to evaluate the hardness of the topcoats. Regarding mechanical properties, impact resistance was also tested. Topcoats' corrosion resistance was assessed using electrochemical impedance spectroscopy (EIS). The stabilization of the corrosion potential in 3.5% NaCl solution was examined by open circuit potential (OCP). Thermogravimetric analysis (TGA) was used to evaluate the thermal stability of differently dried topcoats. Differential scanning calorimetry (DSC) showed the glass transition temperature of the polymer on which the topcoat is based. The degree of crosslinking, which directly affects the mechanical properties of the topcoats, was examined by Fourier-Transform Infrared Spectroscopy (FTIR). This paper compares experimentally obtained properties of atmospherically and IR-dried coatings.

2. Materials and Methods

2.1. Materials and Drying Methods

In this paper, five different topcoats were tested. Their characteristics are presented in Table 1. The table shows the chemical composition, the time required for the topcoat to become dry-to-touch when dried under atmospheric conditions (according to the manufacturer's data sheet and confirmed experimentally), the gloss, and the manufacturer's origin. All the examined topcoats are based on polyurethane (PUR), except for topcoat 2, which is based on polysiloxane (PSX). The times required for the coating to become dry-to-touch vary from 5.5 to 8 h. Tested topcoats 1–4 had a glossy finish, while topcoat 5 had a matte finish. The first three topcoats are of Danish origin, while the other two are of German origin. The examined topcoats are used in the power transformer industry.

Table 1. Characteristics of examined topcoats.

Topcoat	1	2	3	4	5
Chemical composition	PUR	PSX	PUR	PUR	PUR
Dry-to-touch [h]	8	5.5	8	7	6
Gloss	Glossy	Glossy	Glossy	Glossy	Matte
Manufacturer's origin	Danish	Danish	Danish	German	German

The described topcoats were prepared according to the manufacturer's instructions in a mixing bowl. They were applied with a spiral applicator, with the required film thickness according to the manufacturer's technical instructions, on a steel substrate with dimensions 150 × 120 × 18 mm. The substrate was prepared by steel grit blasting to the required cleanliness Sa 2.5, according to ISO 8501-1 [18], and a medium degree of roughness, according to ISO 8503-1 [19]. Half of the applied samples were air-dried, while the other half were dried with infrared (IR) radiation in the cabin for IR drying of liquid coatings owned by the company Končar—Steel structures. The drying chamber consisted of three catalytic gas IR emitters operating at wavelengths from 2 to 10 µm. Substrates with applied topcoats were dried at a distance of 100 cm from the IR emitter. The end of the curing period was detected using a contact method, i.e., a stroke of a pencil. It is considered that the coating is crosslinked when the pencil no longer leaves a mark when lightly stroked over the coating. After the coating had cooled down, a fingernail test was performed to confirm the curing. A properly cured coating should be tack-free and should not scratch [20]. Figure 1 shows a representative view of the dried samples. Topcoats dried in atmospheric conditions are presented in the top row, while the same topcoats dried in an IR cabin are presented in the bottom row.

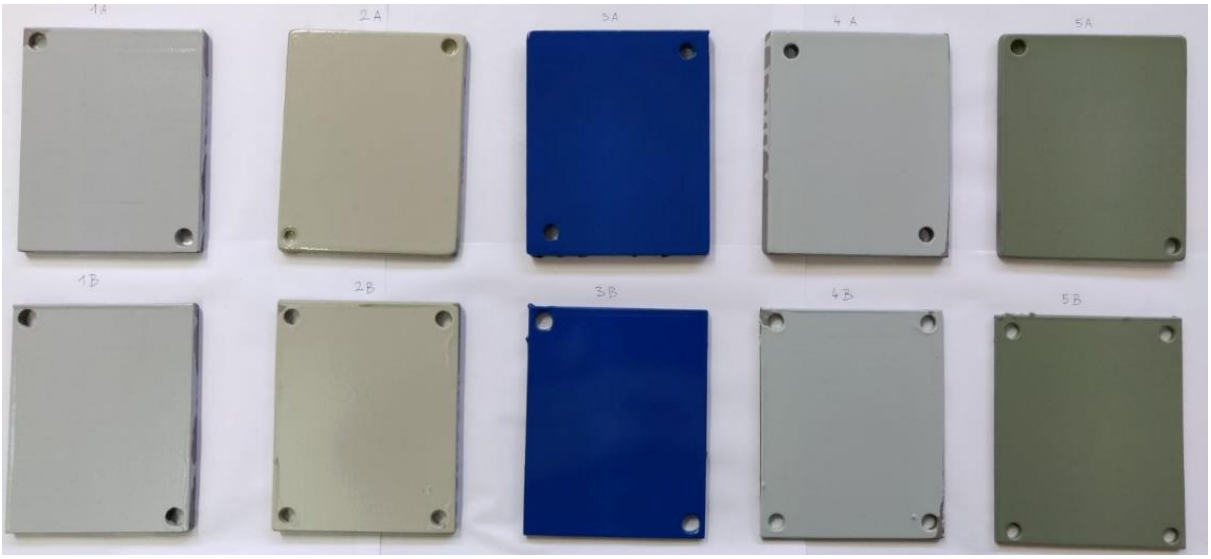


Figure 1. Substrates with topcoats.

2.2. Characterization of Differently Dried Topcoats

2.2.1. Dry Film Thickness, Adhesion, and Gloss

Dry film thickness (DFT) was determined using an Elcometer 456 Coating Thickness Gauge (Elcometer Limited, Edge Lane, Manchester, UK), according to ISO 2808 [21]. Measurements were made at ten different places per sample with instrument accuracy ±2.5 µm, and the mean value was calculated. The adhesion of differently dried coatings to the metal substrate was tested using an Elcometer 510 Automatic Pull-off Adhesion Gauge (Elcometer Limited, Edge Lane, Manchester, UK) with an accuracy of ±1% of full scale,

according to ISO 4624 [22]. The influence of infrared drying on topcoat gloss was examined with an Elcometer 480 Glossmeter (Elcometer Limited, Edge Lane, Manchester, UK) at three different angles, according to ISO 2813 [23]. For both the adhesion and gloss value tests, three measurements were performed, and the mean value was calculated.

2.2.2. Mechanical Properties

The mechanical properties of topcoats were determined using a pencil test and a rapid-deformation (impact resistance) test. To perform the hardness tests, an Elcometer 501 Pencil Hardness Tester (Elcometer Limited, Edge Lane, Manchester, UK) apparatus was used, according to ISO 15184 [24]. The hardness of the hardest pencil that does not leave any mark on the topcoat was recorded as the topcoat scratch hardness. The impact resistance tests were performed according to ISO 6272 [25], using an Elcometer 1615 Variable Impact Tester (Elcometer Limited, Edge Lane, Manchester, UK). A falling-weight test with a large-area indenter and a weight of 1 kg was used. As a result, the drop height (in inches) for which the topcoat did not yet crack was recorded.

2.2.3. Electrochemical Characterization

Electrochemical characterization of the topcoats was performed by measuring the open circuit potential (OCP) and by the electrochemical impedance spectroscopy (EIS) method. The device used for electrochemical measurements was a VersaSTAT 3 Potentiostat/Galvanostat (AMETEK Scientific 131 Instruments, Princeton applied research, Berwyn, PA, USA). Changes in the corrosion potential of a metal substrate with a topcoat in contact with a 3.5% NaCl solution were tested using the open circuit potential [26]. Potential stabilization was carried out for 1000 s with a saturated calomel electrode (SCE) as a reference electrode, at room temperature (23 $\pm$ 2 °C). The corrosion potential of the coated sample was measured after 1, 168, and 240 h spent in the electrolyte. A 3.5% NaCl solution was chosen as the electrolyte because it simulates real conditions from nature, since this is the average concentration of salt in the oceans [26].

Electrochemical impedance spectroscopy was used to assess the chemical resistance of topcoats. Measurements were performed after 1 and 240 h in a 3.5% NaCl solution, at a frequency range of 0.1 to 105 Hz, at room temperature (23 $\pm$ 2 °C), recording 10 points per decade [27]. The tested electrochemical cell consisted of a metal substrate with a topcoat as a working electrode, a saturated calomel electrode as a reference electrode, and two graphite rods as counter electrodes. In order to check the repeatability of the data, each measurement was executed in two replications. Experimental data were analyzed with the AMETEK ZSimpWin program.

2.2.4. Thermogravimetric Analysis (TGA) and Differential Scanning Calorimetry (DSC)

The thermal stability of topcoats was determined with thermogravimetric analysis, using TGA Q500 (TA Instruments, New Castle, DE, USA). Samples weighing around 10 mg were analyzed in a stream of nitrogen (60 mL/min) in the temperature range from −100 to 600 °C with a heating rate of 10 °C/min [28].

A Mettler Toledo differential scanning calorimetry analyzer, DSC822e (Mettler Toledo, Greifensee, Switzerland), was used to determine phase transitions. Samples of about 10 mg were analyzed in a stream of nitrogen (40 mL/min) with a heating and cooling rate of 10 °C/min in the temperature range from −100 °C to 150 °C by a double heating/cooling cycle. Samples were first heated from 25 °C to 150 °C at a rate of 10 °C/min and held at that temperature for 5 min to erase the thermal history of the sample during the preparation process. Samples were then cooled from 150 °C to −100 °C at a cooling rate of 10 °C/min, held at −100 °C for 5 min, and reheated from −100 °C to 150 °C at a rate of 10 °C/min [29]. From the second heating cycle, values of the glass transition temperature Tg were obtained. Liquid nitrogen was used to cool the samples to low temperatures.

2.2.5. Fourier-Transform Infrared Spectroscopy (FTIR)

The chemical composition of topcoats was determined using Fourier-Transform Infrared Spectroscopy (FTIR). A Spectrometer Spectrum One (Perkin Elmer, Waltham, MA, USA) using an Attenuated Total Reflection (ATR) chamber (ZnSe) was used. Measurements were carried out at room temperature in the range of wave numbers 4000–650 cm^{-1} [30]. Topcoat samples were scraped from the metal substrate and recorded in their basic form, without prior preparation.

A flowchart of the described procedures and methods is presented in Figure 2.

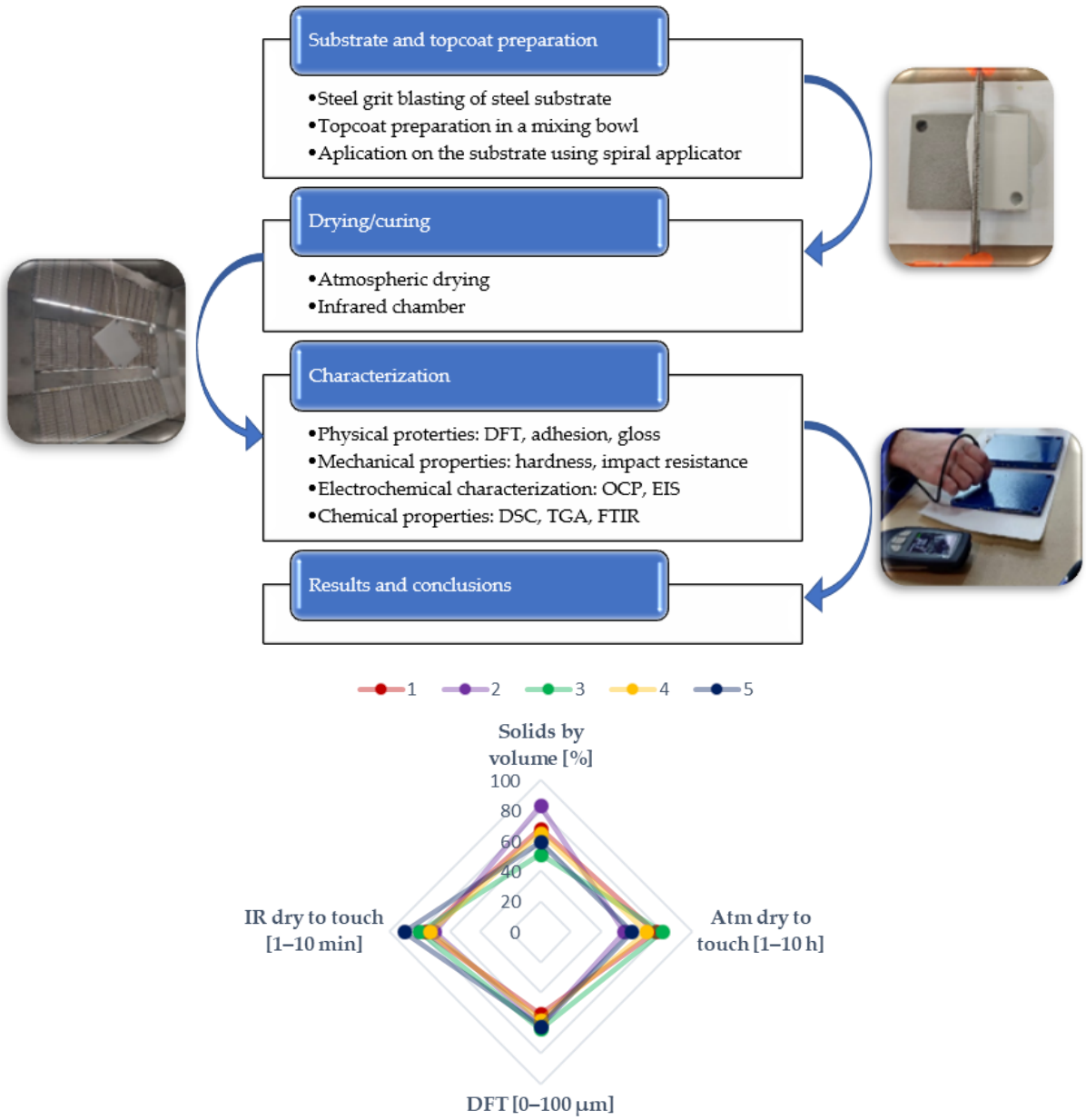


Figure 2. Flowchart of the procedures and methods used in this paper.

3. Results and Discussion

3.1. Drying Time, Dry Film Thickness, Adhesion, and Gloss

According to the manufacturer's data sheet and proven experimentally, topcoats need 5 to 8 h to become dry-to-touch when dried atmospherically. On the other hand, applying IR radiation significantly reduces the drying time, considering that the tested topcoats were dry-to-touch in just 10 min. Regarding dry film thickness, the goal was to obtain a roughly

equal thickness of each film so that the topcoats would be comparable to each other. All samples are within 10 percent of the mean dry film thickness, as shown in Table 2.

Table 2. Type of drying (under atmospheric conditions—atm, applying infrared radiation—IR), time required for the topcoat to be dry-to-touch, dry film thickness, and pull-off values of differently dried topcoats.

Topcoat	Type of Drying	Drying Time [min]	DFT [µm]	Pull-Off [MPa]
1	atm	480	62.8	11.2
	IR	10	65.9	19.4
2	atm	330	62.4	16.1
	IR	10	60.3	19.2
3	atm	480	62.1	17.2
	IR	10	65.7	24.8
4	atm	420	58.1	11.4
	IR	10	60.8	8.2
5	atm	360	63.8	7.6
	IR	10	63.7	10.4

Pull-off adhesion values, which are also shown in Table 2, are higher when applying IR radiation. This means that the adhesion of the coating to the substrate is better when the coating is dried with IR radiation. The explanation of this effect lies in better crosslinking of the polymer when using IR radiation for curing, due to which the resistance to the tensile load applied in the pull-off adhesion test is better, and the topcoat has higher tensile strength [31]. A representative view of pull-off values is shown in Figure 3.

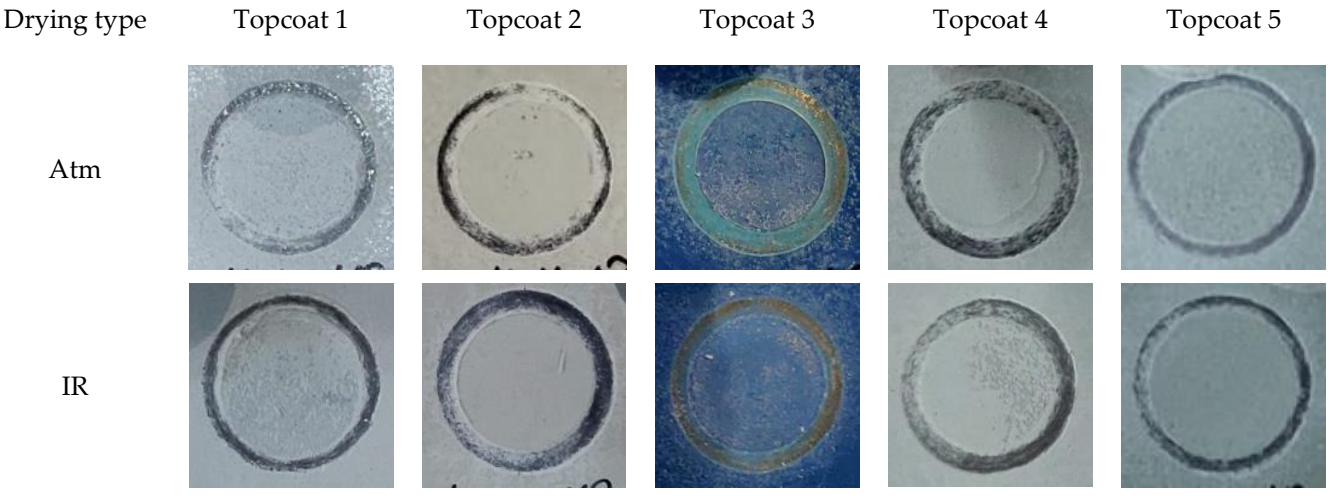
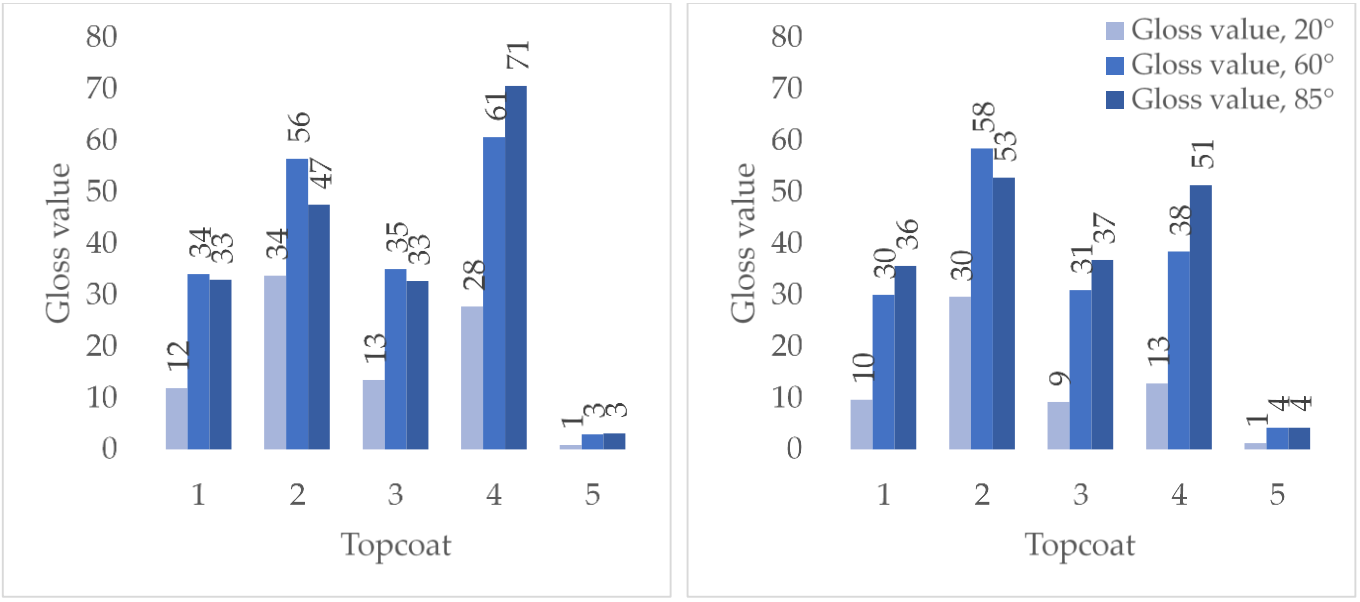


Figure 3. Representative pull-off values for each topcoat.

The gloss values of five tested topcoats, at three different angles, are shown graphically in Figure 4. Figure 4a shows gloss values of atmospherically dried topcoats, while graph Figure 4b shows gloss values of infrared-dried topcoats. Values obtained at different angles mostly match, regardless of the drying method. The only slightly larger deviation is with topcoat 4, whose gloss values are higher in the case of atmospheric drying. The lowest gloss values were recorded for topcoat 5, which is matte. Such low gloss values were expected.



(**a**) (**b**)

Figure 4. Gloss values at different angles for (**a**) atmospherically and (**b**) IR-dried topcoats.

3.2. Mechanical Properties

Coatings that have higher hardness resist wear better [32]. Also, good impact resistance is desirable, since it describes the coating's ability to absorb impact energy without breaking [33]. The scratch hardness of the examined topcoats was determined with a pencil test, and the results are shown in Table 3. All of the topcoats show similar scratch hardness, around HB. In two cases, IR-dried topcoats show higher hardness than the air-dried ones, while in other cases, the hardness is the same. The results of the impact test differ. Topcoats based on polysiloxane showed the lowest impact resistance. Polyurethane-based topcoats show better impact resistance. Some topcoats showed no plastic deformation, even when the drop height was at the highest level (which is limited by the apparatus). In half of the cases, the impact resistance was slightly better for atmospherically dried topcoats, while in the other half, it was somewhat better in the case of IR drying. That means that the drying method has no significant influence on the impact resistance of the topcoat.

Table 3. Pencil hardness and impact resistance of differently dried topcoats.

Topcoat	Type of Drying	Scratch Hardness	Impact Resistance [in]
1	atm	HB	33
	IR	HB	28
2	atm	HB	7
	IR	F	10
3	atm	HB	40 *
	IR	HB	40 *
4	atm	B	19
	IR	F	21
5	atm	HB	40 *
	IR	HB	36

* Topcoats did not crack even when the drop height was at the highest level.

3.3. Electrochemical Characterization

The results of measuring the open circuit potential after stabilization in 3.5% NaCl solution are shown in Table 4. Measurements after 1 hour differ significantly from the measurements after 168 h (7 days) and 240 h (10 days), which means that the corrosion potential did not stabilize after 1 hour spent in the electrolyte. The results of measuring the corrosion potential after 168 and 240 h are similar, which indicates the stabilization of the corrosion potential of the coated sample.

Table 4. Open circuit potential after stabilization in a 3.5% NaCl solution.

Topcoat	E_{corr} vs. SCE [mV]		
	1 h	**168 h**	**240 h**
1 IR	−464.9	−195.4	−202.7
1 atm	−513.4	−333.7	−288.3
2 IR	−46.0	−217.8	−216.3
2 atm	−540.1	−102.1	−258.6
3 IR	−138.9	−214.1	−151.8
3 atm	−562.2	−201.2	−241.4
4 IR	49.4	−182.5	−140.8
4 atm	200.9	−433.1	−360.7
5 IR	−432.1	−179.1	−169.6
5 atm	−559.7	−135.9	−127.0

Equivalent electrical circuits used to describe EIS results are shown in Figure 5a,b. Circuits consist of electrolyte resistance (R_s), coating resistance (R_c), coating capacitance (C_c), charge transfer resistance (R_{ct}), and double-layer capacitance between metal and electrolyte solution (C_{dl}). In some cases, an ideal capacitor model (C) was used to describe the capacitor, while in some other cases, the results were better described by a constant phase element (Q), which represents an imperfect capacitor. After 10 days in the electrolyte, with the 1 atm, 1 IR, and 2 atm topcoats, diffusion of the electrolyte to the metal substrate occurred, so the equivalent circuit in Figure 5b was used. This circuit contains an additional element W, i.e., Warburg impedance, which describes the phenomenon of diffusion [5,30].

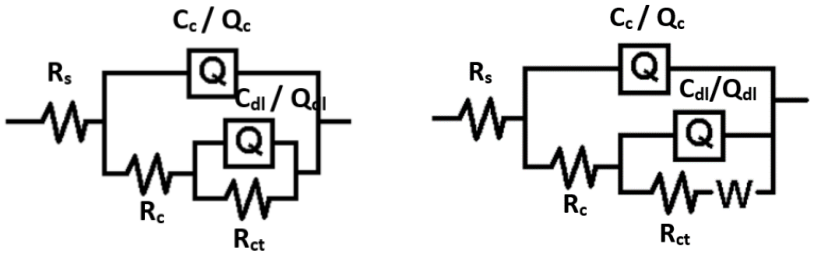


Figure 5. Equivalent electric circuit models: (**a**) electric circuit with three resistors and two capacitors, (**b**) the same circuit with the addition of element W, Warburg impedance [5].

Numerical values of coating resistance that were calculated using the ZSimpWin program are shown in Figure 6. Nyquist and Bode plots obtained by mathematical models, according to equivalent electric circuits, are shown in Figures 7 and 8. The IR-dried samples initially showed higher resistance than the air-dried samples. After exposure to the electrolyte, topcoats 1 and 2 show greater stability when IR-dried, while the other topcoats show greater stability in the case of atmospheric drying. Resistance of the coating decreased

after ten days of exposure to the electrolyte, probably because of the penetration of the electrolyte into the micropores of the coating. Topcoat 1's protective properties deteriorated the most. This was probably due to a too-low film thickness, as the optimal thickness of the dry film is 100 µm, according to the manufacturer's recommendations. After one hour of immersion in the electrolyte, the PSX-based topcoat showed the best corrosion resistance. After ten days in the electrolyte, its resistance remained high. Topcoat 4 showed the highest resistance after 10 days. According to its technical data sheet, this topcoat has active pigments in its composition. Active pigments reduce or prevent corrosion of the metal substrate electrochemically by a galvanic or passivating mechanism or by building-up solid compounds with barrier properties that plug the damage in the coating [34].

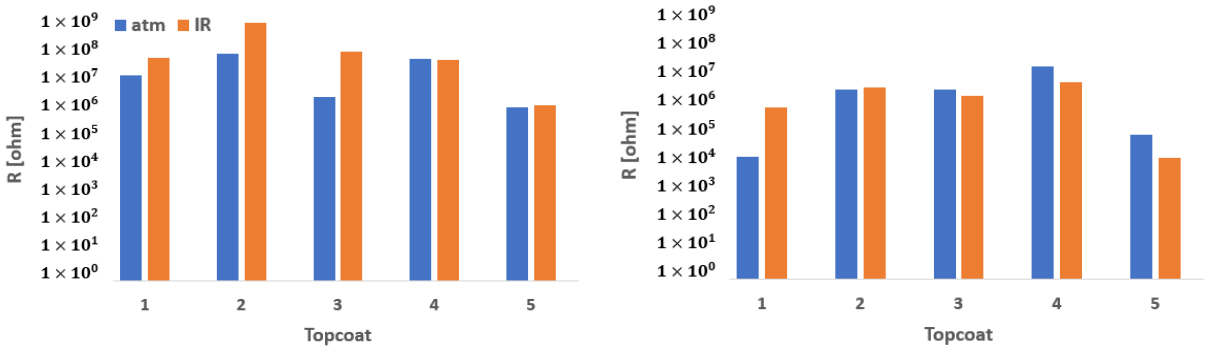


Figure 6. Topcoats resistance after 1 h (**a**) and 240 h (**b**) in 3.5% NaCl solution.

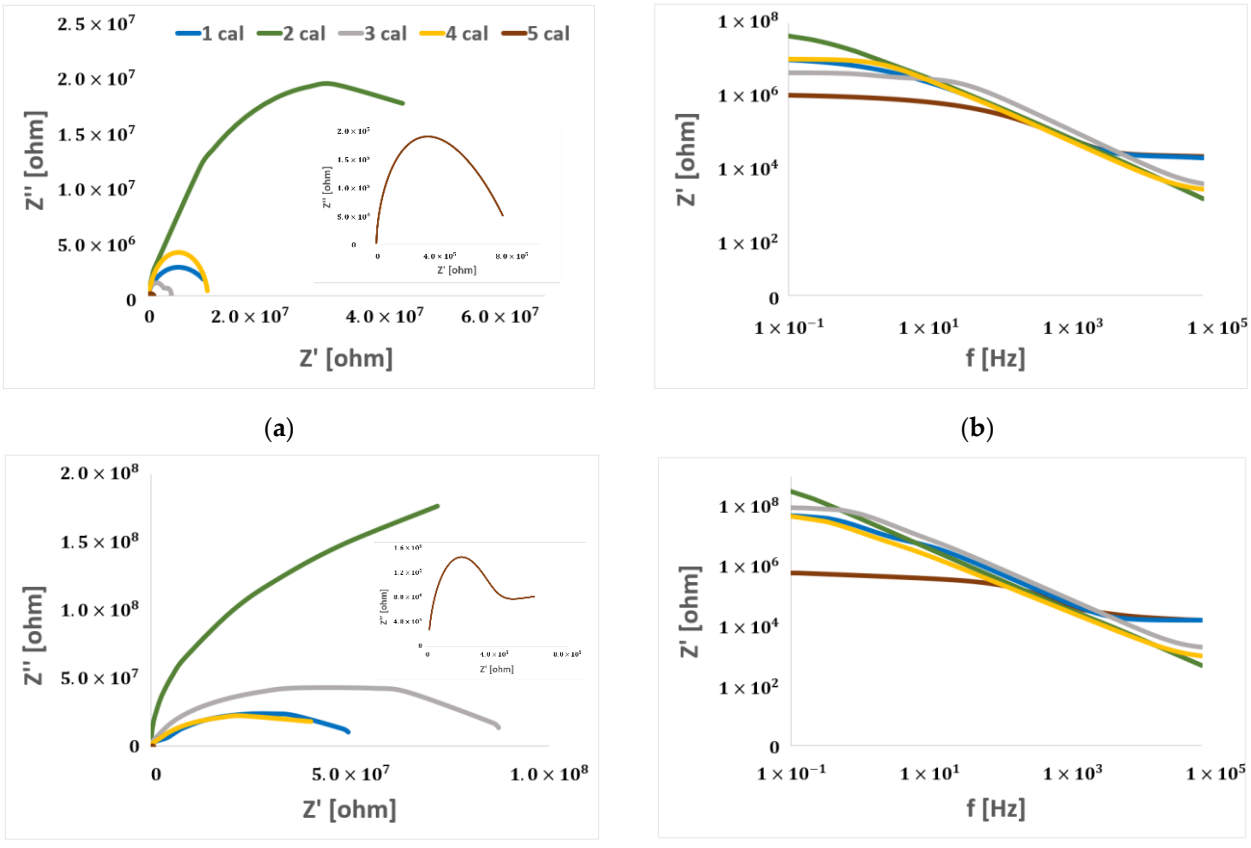


Figure 7. Nyquist and Bode plots for topcoats dried atmospherically (**a**,**b**) and with IR radiation (**c**,**d**) after 1 h in 3.5% NaCl solution.

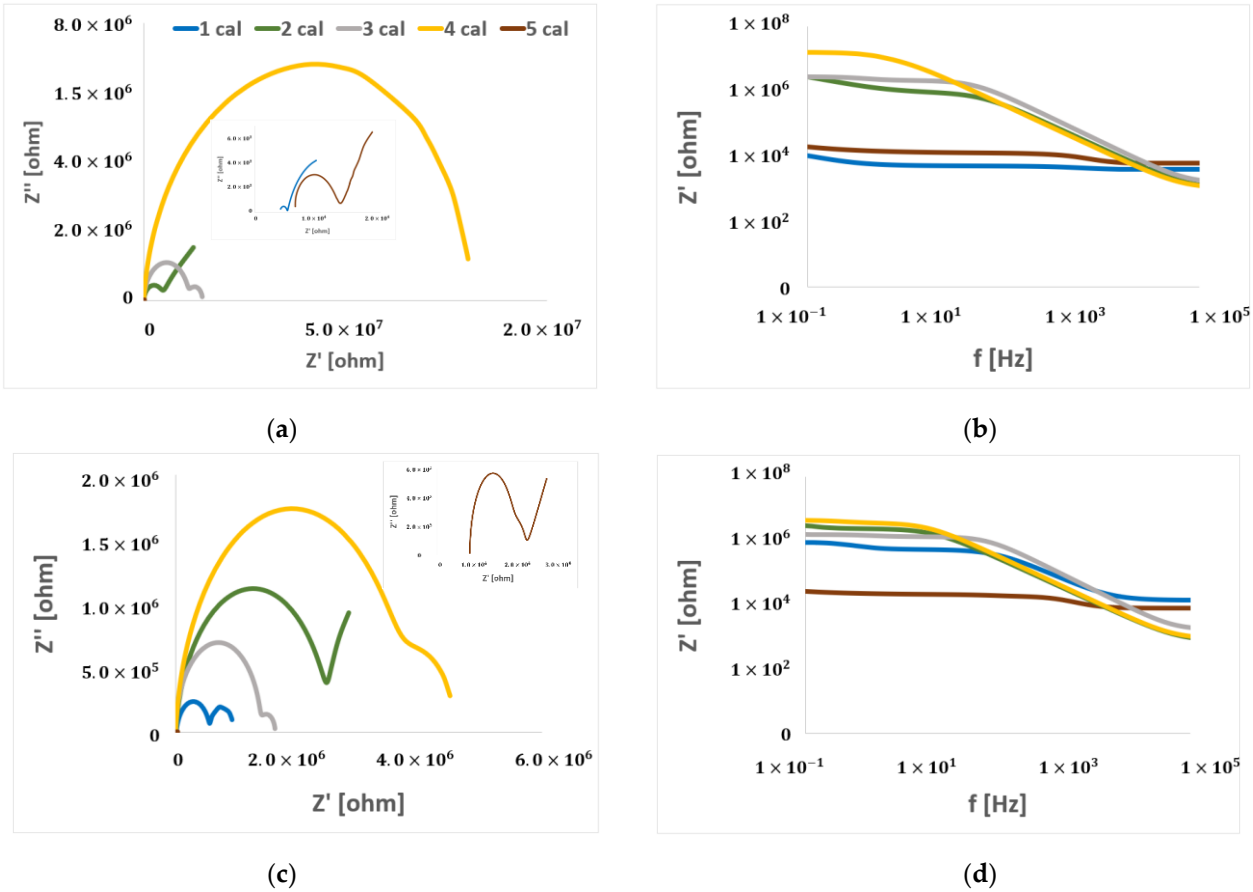


Figure 8. Nyquist and Bode plots for topcoats dried atmospherically (**a**,**b**) and with IR radiation (**c**,**d**) after 240 h in 3.5% NaCl solution.

3.4. Thermogravimetric Analysis (TGA) and Differential Scanning Calorimetry (DSC)

From TG and DTG curves, obtained by thermogravimetric analysis, the following features were determined: temperature at the beginning of decomposition ($T_{5\%}$) at 5% mass loss and temperature at the end of decomposition (T_f), as shown in Table 5. The initial decomposition temperature was, in most cases, higher in the case of IR-drying, which indicates the higher thermal stability of topcoats dried with IR radiation [35]. Only topcoat 5 showed better thermal stability when dried atmospherically. Topcoat 5's technical data sheet states that there is a presence of special barrier pigments in its composition. Some barrier pigments have reflective properties to avoid unnecessary heating [36]. Instead of absorbing the infrared energy, they reflect it back, reducing the amount of heat generated during the curing process, which can affect the curing kinetics and, consequently, the thermal stability. TGA thermograms of examined topcoats are shown in Figure A1.

The result of differential scanning calorimetry is the glass transition temperature, T_g, of the polymer (Table 5). Higher T_g values are desirable since they indicate better curing of the polymer [31,37]. As the curing of the polymer progresses, the molecular network mobility decreases; the degree of crystallinity increases; and the glass transition temperature of the polymer, T_g, increases with it. In the case of PUR-based topcoats, T_g is higher in the case of IR-drying, while a PSX-based topcoat (topcoat 2) exhibits a higher T_g value when dried atmospherically. Infrared radiation can have two effects on the glass transition of polymers. First is the heating effect, in which IR radiation transfers energy to the polymer, resulting in an increase in temperature. With higher curing temperature, the degree of crosslinking and the glass transition temperature increase [38]. That is the case with all examined PUR topcoats. On the other hand, the PSX-based topcoat (topcoat 2) has the shortest drying time, according to its technical data sheet. This latter was exposed to infrared radiation for

the same amount of time as PUR-based topcoats. The PSX might require a shorter period of exposure to IR radiation because infrared radiation induces polymer scission, which increases the mobility of the polymer chains, and as a result of that, the glass transition temperature decreases [39]. DSC thermograms for the second heating cycle are shown in Figure A2.

Table 5. Results obtained by TGA ($T_{5\%}$, T_f) and DSC analyses (T_g).

Topcoat	$T_{5\%}$ [°C]	T_f [°C]	T_g [°C]
1 atm	252.9	437.6	39.4
1 IR	254.7	438.1	45.0
2 atm	257.6	536.0	85.7
2 IR	259.3	536.0	81.2
3 atm	226.4	391.3	39.8
3 IR	236.1	388.0	43.2
4 atm	263.8	474.3	37.6
4 IR	267.9	460.0	41.3
5 atm	268.1	413.3	45.5
5 IR	261.8	402.0	56.1

3.5. Fourier-Transform Infrared Spectroscopy (FTIR)

Table 6 gives an overview of the peak positions recorded by ATR-FTIR and a description of the characteristic absorption bands for polyurethanes. Walo et al. [28] state that absorption bands (recorded for atmospherically dried topcoats 1 and 3) at 3457.24 and 3457.58 cm^{-1} characterize free N-H stretching, while absorption bands (recorded for IR-dried topcoats 1 and 3) at 3382.27 and 3372.84 cm^{-1} characterize hydrogen-bonded N-H stretching. Similarly, Li et al. [29] state that absorption bands (of atmospherically dried topcoats 1 and 3) at 1737.06 and 1734.32 cm^{-1} characterize free urethano, while absorption bands (of IR-dried topcoats 1 and 3) at 1721.69 and 1722.90 cm^{-1} characterize hydrogen-bonded urethano. Hydrogen bonds explain the better mechanical properties of IR-cured topcoats, given that the intermolecular forces generated by them can improve the crosslinking density of polymers [29]. For topcoats 4 and 5, these wave numbers differ less, regardless of the drying method. FTIR spectra of PUR-based topcoats are shown in Figure A3, and the FTIR spectrum of the PSX-based topcoat is shown in Figure A4.

Table 6. Peak positions recorded on the ATR-FTIR spectrum and characteristic absorption bands for polyurethanes explained [40,41].

Wavenumber [cm^{-1}]								Assignment
Topcoat 1		Topcoat 3		Topcoat 4		Topcoat 5		
atm	IR	atm	IR	atm	IR	atm	IR	
3736.48	3738.29		3736.24	3677.26	3677.40			O-H stretching
3457.58	3382.27	3457.24	3372.84	3371.98	3367.21	3365.08	3380.38	N-H stretching
2955.58	2929.27	2941.43	2930.34	2928.97	2928.88	2929.56	2929.53	C-H asymmetric stretching
2864.64	2862.15	2869.03	2866.86	2860.18	2860.24	2859.81	2859.13	C-H symmetric stretching
1737.06	1722.90	1734.32	1721.69	1724.49	1723.25	1725.34	1724.99	C=O stretching vibrations interacting with H bond urethane
1443.11	1449.88	1448.57	1452.53	1461.47	1460.05	1452.89	1453.02	CH_2 scissoring and CH_3 deformation
		1115.85						Free C-O-C stretching
1082.86	1081.24	1071.56	1067.21	1073.40	1072.60	1073.10	1073.76	H bound C-O-C stretching

Table 7 gives an overview of the peak positions recorded by ATR-FTIR and a description of the characteristic absorption bands for polysiloxanes. Atmospherically and IR-dried topcoats show absorption peaks at similar wavelengths, with the exception of the absorption peak of the IR-cured topcoat at 1064.24 cm^{-1}. This peak indicates the asymmetric stretching of the Si-O-Si groups with a higher crosslinking degree [42]. The absence of a peak at that wavelength of the atmospherically dried topcoat indicates a lower degree of crosslinking of that topcoat, thus explaining the poorer mechanical properties of this coating, which was confirmed by the pencil and impact resistance tests.

Table 7. Peak positions recorded on the ATR-FTIR spectrum and characteristic absorption bands for polysiloxanes explained [42].

Wavenumber [cm^{-1}]		**Assignment**
Topcoat 2		
atm	**IR**	
1258.34	1259.31	CH_3 symmetric bending
	1064.24	Si-O-Si asymmetric stretching (high crosslinking degree)
1018.59	1021.55	Si-O-Si asymmetric stretching (surface groups, low crosslinking degree)
844.76	845.46	Si-CH_3 vibration
798.99	799.40	Si-C vibration

4. Conclusions

The results of this study showed overall better properties of infrared-dried industrial topcoats in relation to the same topcoats dried under atmospheric conditions. In addition to better crosslinking of polymers, which results in better protective properties of the topcoat, drying times are significantly shortened, which is especially important from an industrial point of view. Conclusions based on the conducted tests are as follows:

- Pull-off adhesion values are higher when applying IR radiation to cure the topcoat.
- Gloss values remain similar, regardless of the drying method. Furthermore, no changes in the shade of the topcoat are visible to the eye.
- Topcoat hardness is equal or higher in the case of IR-drying, while differently dried topcoats show a similar impact resistance.
- EIS initially showed a higher resistance of the IR-dried coatings. After 10 days in the electrolyte, topcoats from the Danish manufacturer show similar or better resistance in the case of IR drying, while IR-dried topcoats from the German manufacturer show a slightly lower resistance than the atmospherically dried ones.
- TGA showed a better thermal stability of IR-cured topcoats.
- DSC results showed that the glass transition temperature of the PUR-based topcoat increases when infrared radiation is applied, while the glass transition temperature of PSX decreases with the application of IR radiation, which indicates the sensitivity of PSX to IR radiation and the possible polymer scission effect.
- The results of FTIR indicate a higher curing degree of IR-dried topcoats.
- Although, in principle, infrared radiation improves the properties of the coating, it is necessary to pay attention to both the base polymer in the coating and the existence of special fillers or pigments that can affect the curing of the coating.

Author Contributions: M.L. and I.F. performed the experiments; V.A. analyzed the data; M.L. wrote the paper; I.S. designed the experiments and revised and edited the paper; D.R.-R. provided resources and the drying experimental setup. All authors have read and agreed to the published version of the manuscript.

Funding: This study is based on a project "Smart plant for drying liquid coatings", which is co-financed within the Operational Programme Competitiveness and Cohesion from the European Regional Development Fund under reference number KK.01.2.1.02.0030.

Institutional Review Board Statement: Not applicable.

Informed Consent Statement: Not applicable.

Data Availability Statement: Not applicable.

Conflicts of Interest: The authors declare no conflict of interest.

Appendix A

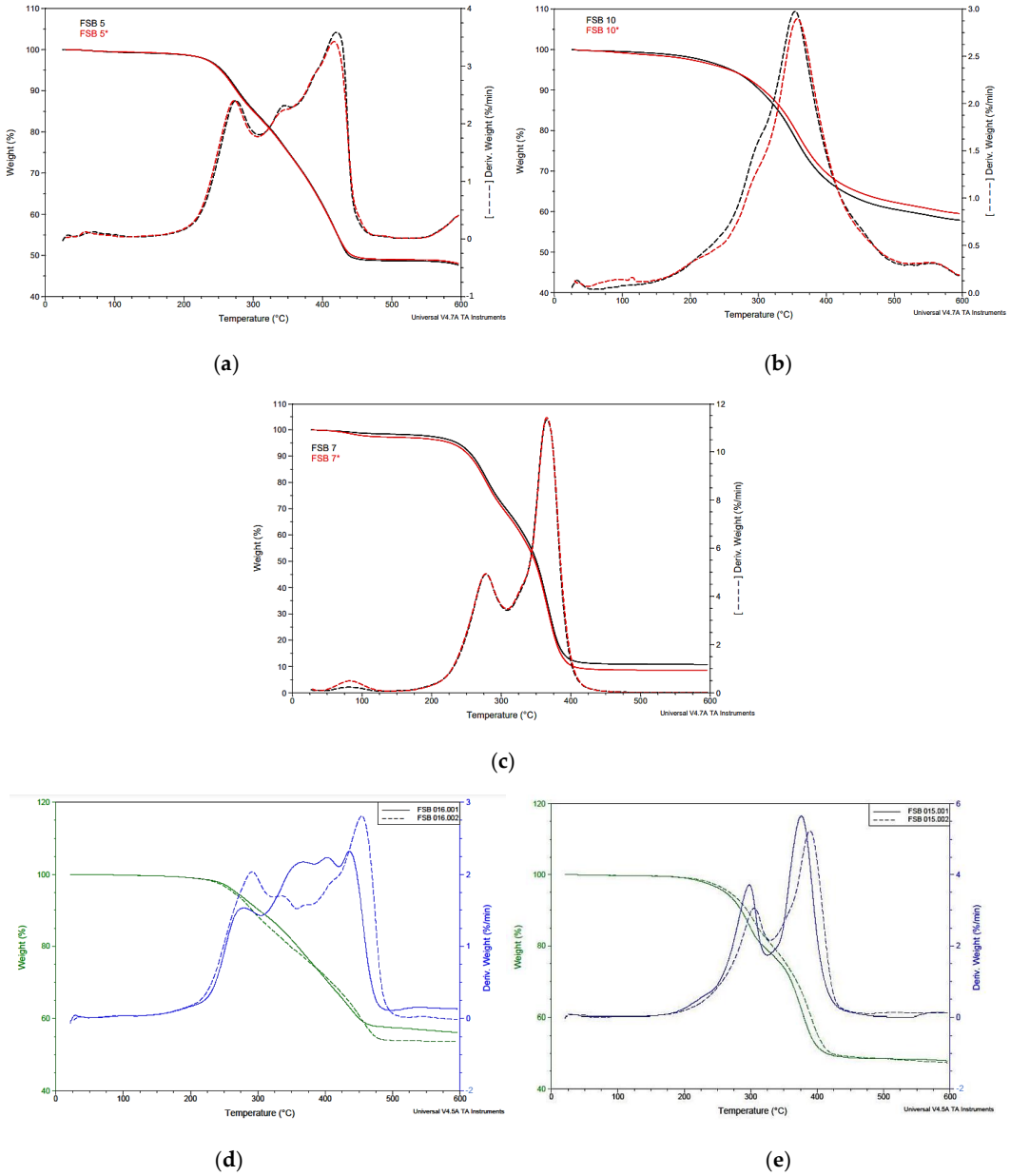


Figure A1. TGA thermograms of topcoats 1 (**a**), 2 (**b**), 3 (**c**), 4 (**d**), and 5 (**e**). Graphs obtained for topcoats from Danish manufacturer (1, 2, 3) that are dried atmospherically are colored red, and IR-dried topcoats are colored black. Graphs obtained for topcoats from German manufacturer (4, 5) that are dried atmospherically are marked on the graph with dashed lines, and IR-dried topcoats are marked with a solid line.

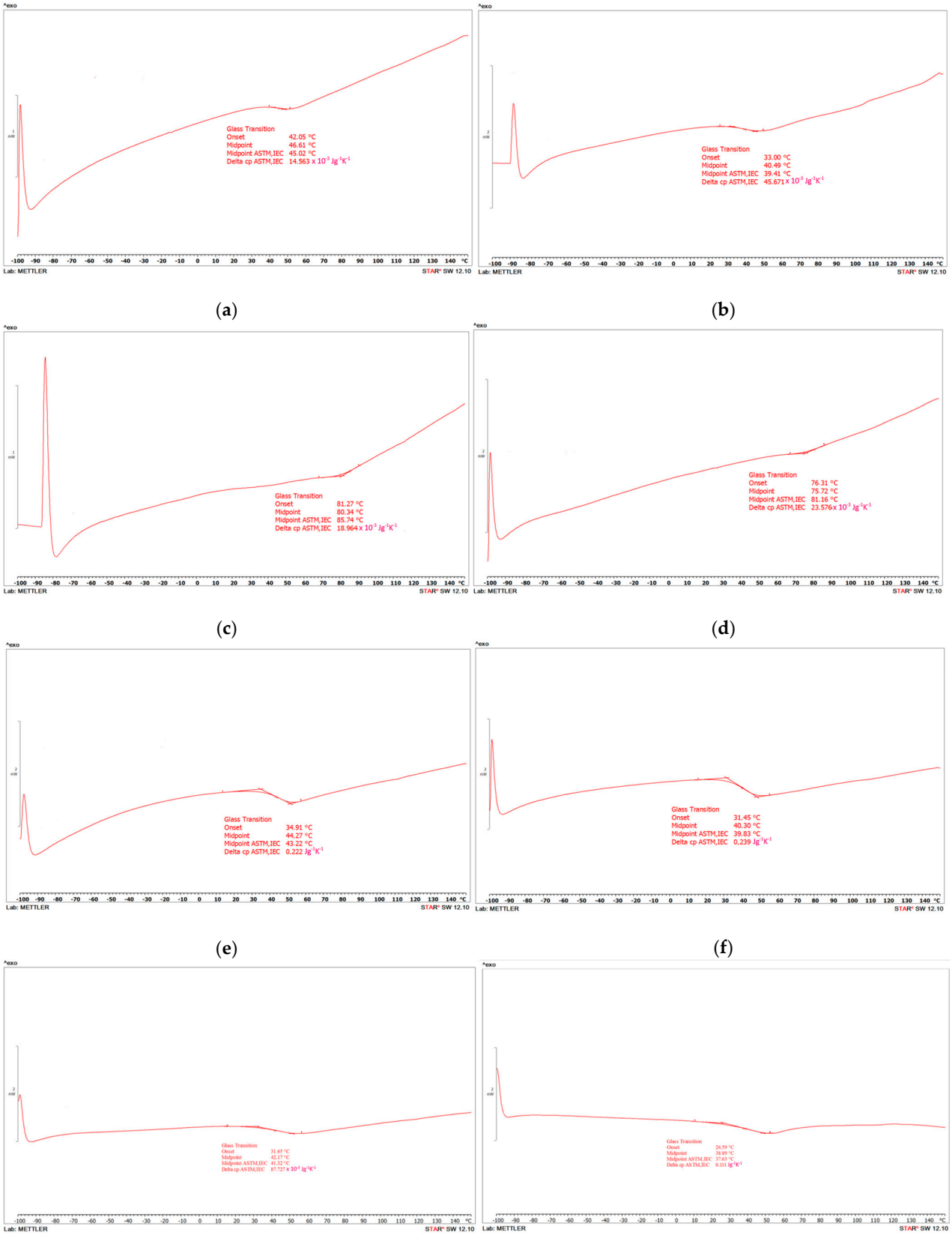
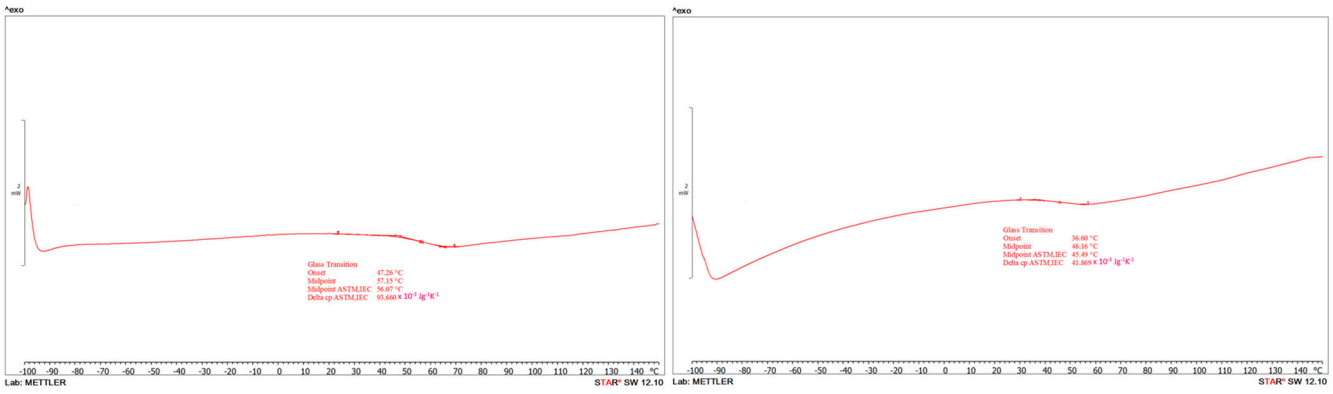
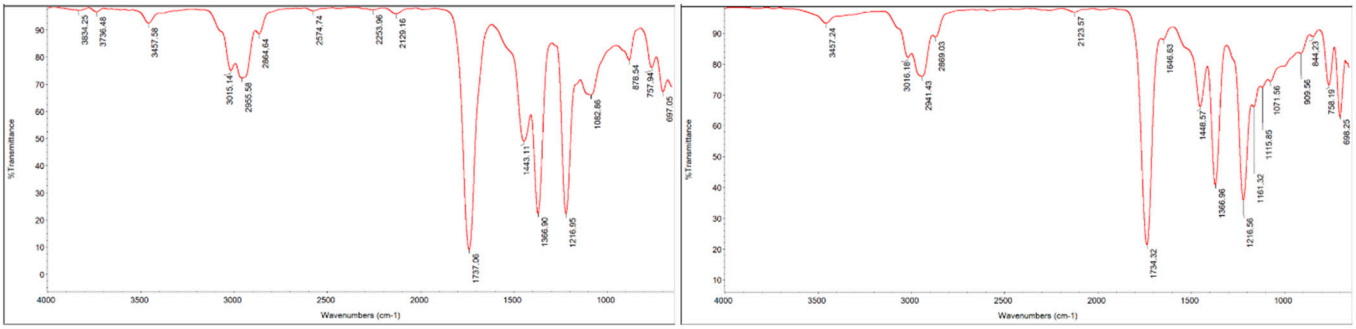


Figure A2. *Cont.*

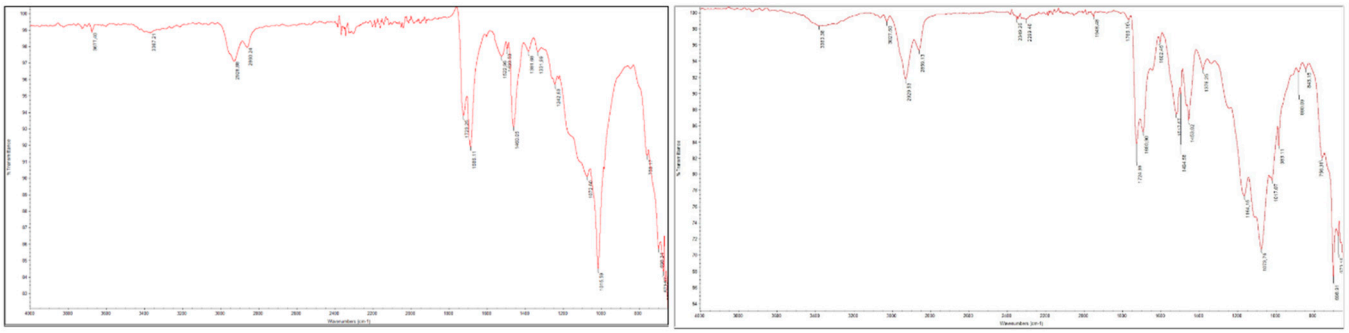


(**i**) (**j**)

Figure A2. DSC thermograms for topcoat 1 IR-dried (**a**) and atm-dried (**b**), topcoat 2 IR-dried (**c**) and atm-dried (**d**), topcoat 3 IR-dried (**e**) and atm-dried (**f**), topcoat 4 IR-dried (**g**) and atm-dried (**h**), and topcoat 5 IR-dried (**i**) and atm-dried (**j**).



(**a**) (**b**)



(**c**) (**d**)

Figure A3. FTIR spectra of topcoats 1 (**a**), 3 (**b**), 4 (**c**), and 5 (**d**).

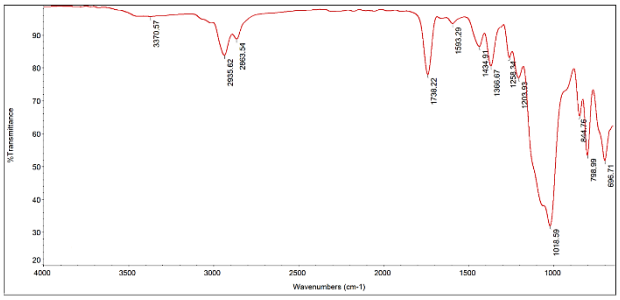


Figure A4. FTIR spectrum of topcoat 2.

References

1. Valdez, B.; Schorr, M.; Zlatev, R.; Carrillo, M.; Stoytcheva, M.; Alvarez, L.; Eliezer, A.; Rosas, N. Corrosion Control in Industry. In *Environmental and Industrial Corrosion—Practical and Theoretical Aspects*; Valdez, B., Schorr, M., Eds.; InTech: Rijeka, Croatia, 2012; Volume 1, pp. 19–51. [CrossRef]
2. NACE International. Economic Impact. Available online: http://impact.nace.org/economic-impact.aspx (accessed on 19 April 2023).
3. Hinton, B.R.W. Corrosion prevention and control. In *Handbook on the Physics and Chemistry of Rare Earths*; Gischneidner, K.A., Jr., Eyring, L., Eds.; North-Holland: Amsterdam, The Netherlands, 1995; Volume 21, pp. 29–35. [CrossRef]
4. Maaß, P. Corrosion and Corrosion Protection. In *Handbook of Hot-Dip Galvanization*; Maaß, P., Peißker, P., Eds.; Wiley-VCH: Weinheim, Germany, 2011; Volume 1, pp. 1–19. [CrossRef]
5. Alsamuraee, A.M.A.; Jaafer, I.H.; Ameen, A.H.; Abdullah, Q.A. Electrochemical impedance spectroscopic evaluation of corrosion protection properties of polyurethane/polyvinyl chloride blend coating on steel. *Am. J. Sci. Res.* **2011**, *2*, 761–768. [CrossRef]
6. Zheng, S.X. *Principles of Organic Coatings and Finishing*, 1st ed.; Cambridge Scholars Publishing: Newcastle upon Tyne, UK, 2020; pp. 1–14. Available online: https://www.cambridgescholars.com/resources/pdfs/978-1-5275-4119-1-sample.pdf (accessed on 7 June 2023).
7. Davidson, R.S.; Holman, R.J. Developments and trends in radiation curing. *Rev. Prog. Color.* **2003**, *33*, 46–58. [CrossRef]
8. Nienhuis, J.G. *Review on Drying and Curing Techniques of Coatings*; SHR: Wageningen, The Netherlands, 2004. Available online: http://virtual.vtt.fi/virtual/proj6/coste18/nienhuisdryingpaper.pdf (accessed on 7 June 2023).
9. Wali, A.S.; Kumar, S.; Khan, D. A review on recent development and application of radiation curing. *Mater. Today Proc.* **2023**, *82*, 68–74. [CrossRef]
10. Florencia, M.; López, A.; Barbosa, S.E.; Martini, R.E. Use of infrared radiation as curing agent for bioactive paper fabrication in times compatible with industrial process. *Chem. Eng. Process. Process Intensif.* **2020**, *157*, 108165. [CrossRef]
11. Pendar, M.-R.; Rodrigues, F.; Páscoa, J.C.; Lima, R. Review of coating and curing processes: Evaluation in automotive industry. *Phys. Fluids.* **2022**, *34*, 101301. [CrossRef]
12. Pathania, A.; Arya, R.K.; Ahuja, S. Crosslinked polymeric coatings: Preparation, characterization, and diffusion studies. *Prog. Org. Coat.* **2017**, *105*, 149–162. [CrossRef]
13. Saure, R.; Gnielinski, V. Moisture measurement by FT-IR-spectroscopy. *Dry. Technol.* **1994**, *12*, 1427–1444. [CrossRef]
14. Saure, R.; Wagner, G.R.; Schlunder, E.U. Drying of solvent-borne polymeric coatings. II. Experimental results using FTIR spectroscopy. *Surf. Coat. Technol.* **1998**, *99*, 257–265. [CrossRef]
15. Geipel, C.; Stephan, P. Experimental investigation of the drying process of automotive base paints. *Appl. Therm. Eng.* **2005**, *25*, 2578–2590. [CrossRef]
16. Vessot, S.; Andrieu, J.; Laurent, P.; Galy, J.; Gerard, J.F. Air convective drying and curing of polyurethane-based paints on sheet molding compound surfaces. *J. Coat. Technol.* **1998**, *70*, 67–76. [CrossRef]
17. Stojanović, I.; Cindrić, I.; Janković, L.; Šimunović, V.; Franjić, H. Performance Assessment of Differently Dried Coating Systems for Corrosion Prevention in Power Transformer Industry. *Coatings* **2021**, *12*, 331. [CrossRef]
18. *ISO 8501-1*; Preparation of Steel Substrates before Application of Paints and Related Products—Visual Assessment of Surface Cleanliness—Part 1: Rust Grades and Preparation Grades of Uncoated Steel Substrates and of Steel Substrates after Overall Removal of Previous Coatings. International Organization for Standardization: Geneva, Switzerland, 2007.
19. *ISO 8503-1*; Preparation of Steel Substrates before Application of Paints and Related Products—Surface Roughness Characteristics of Blast-Cleaned Steel Substrates—Part 1: Specifications and Definitions for ISO Surface Profile Comparators for the Assessment of Abrasive Blast-Cleaned Surfaces. International Organization for Standardization: Geneva, Switzerland, 2012.
20. Jonkers, G.; Nienhuis, J.G.; van de Velde, B. Climate Independent Painting: Is Infrared Heating a Solution for Professional Painters? *Macromol. Symp.* **2002**, *187*, 249–260. [CrossRef]
21. *ISO 2808*; Paints and Varnishes—Determination of Film Thickness. International Organization for Standardization: Geneva, Switzerland, 2019.
22. *ISO 4624*; Paints and Varnishes—Pull-Off Test for Adhesion. International Organization for Standardization: Geneva, Switzerland, 2016.
23. *ISO 2813*; Paints and Varnishes—Determination of Gloss Value at 20°, 60° and 85°. International Organization for Standardization: Geneva, Switzerland, 2014.
24. *ISO 15184*; Paints and Varnishes—Determination of Film Hardness by Pencil Test. International Organization for Standardization: Geneva, Switzerland, 2020.
25. *ISO 6272*; Paints and Varnishes—Rapid-Deformation (Impact Resistance) Tests—Part 1: Falling-Weight Test, Larne-Area Indenter. International Organization for Standardization: Geneva, Switzerland, 2002.
26. Wright, J.M.; Colling, A. *Seawater: Its Composition, Properties and Behaviour*, 2nd ed.; Butterworth-Heinemann: Oxford, UK, 1995; p. 5. [CrossRef]
27. Samardžija, M.; Alar, V.; Špada, V.; Stojanović, I. Corrosion Behaviour of an Epoxy Resin Reinforced with Aluminium Nanoparticles. *Coatings* **2022**, *12*, 1500. [CrossRef]
28. Walo, M.; Przybytniak, G.; Kavakli, P.A.; Güven, O. Radiation-induced graft polymerization of N-vinylpyrrolidone onto segmented polyurethane based on isophorone diisocyanate. *Radiat. Phys. Chem.* **2013**, *84*, 85–90. [CrossRef]

29. Li, S.; Liu, Z.; Hou, L.; Chen, Y.; Xu, T. Effect of polyether/polyester polyol ratio on properties of waterborne two component polyurethane coatings. *Prog. Org. Coat.* **2020**, *141*, 105545. [CrossRef]
30. Šoić, I.; Martinez, S.; Dubravić, M. Gel-Electrolyte EIS setup used for probing of IR Dried/Cured industrial coatings. *Prog. Org. Coat.* **2019**, *137*, 105331. [CrossRef]
31. Uday, M.; Kiran Kumar, P. Heat transfer studies for infrared radiation assisted curing in polymer composites. *J. Phys. Conf. Ser.* **2020**, *1473*, 12027. [CrossRef]
32. Bai, H.; Zhong, L.; Kang, L.; Liu, J.; Zhuang, W.; Lv, Z.; Xu, Y. A review on wear-resistant coating with high hardness and high toughness on the surface of titanium alloy. *J. Alloys Compd.* **2021**, *882*, 160645. [CrossRef]
33. DeArmitt, C. Functional Fillers for Plastics. In *Applied Plastics Engineering Handbook*, 2nd ed.; Kutz, M., Ed.; William Andrew Publishing: Norwich, NY, USA, 2017; Volume 3, pp. 517–532. [CrossRef]
34. Rammelt, U.; Reinhard, G. Characterization of active pigments in damage of organic coatings on steel by means of electrochemical impedance spectroscopy. *Prog. Org. Coat.* **1994**, *24*, 309–322. [CrossRef]
35. Kuźnia, M.; Magiera, A.; Zygmunt-Kowalska, B.; Kaczorek-Chrobak, K.; Pielichowska, K.; Szatkowski, P.; Benko, A.; Ziąbka, M.; Jerzak, W. Fly Ash as an Eco-Friendly Filler for Rigid Polyurethane Foams Modification. *Materials* **2021**, *14*, 6604. [CrossRef]
36. Coser, E.; Froes Moritz, V.; Krezinger, A.; Ferreire, C.A. Development of paints with infrared radiation reflective properties. *Polímeros* **2015**, *25*, 305–310. [CrossRef]
37. Acik, G.; Karabulut, H.R.F.; Altinkok, C.; Karatavuk, A.O. Synthesis and characterization of biodegradable polyurethanes made from cholic acid and L-lysine diisocyanate ethyl ester. *Polym. Degrad. Stab.* **2019**, *165*, 42–48. [CrossRef]
38. Michel, M.; Ferrier, E. Effect of curing temperature conditions on glass transition temperature values of epoxy polymer used for wet lay-up applications. *Constr. Build. Mater.* **2020**, *231*, 117206. [CrossRef]
39. Al-Qaraqawi, I.Y.; Abdulmalik, D.A.; Madi, N.K.; Almaadeed, M. Gamma irradiation effects on polymethyl methacrylate. *Phys. Stat. Sol.* **2007**, *4*, 3727–3730. [CrossRef]
40. Mora-Murillo, L.D.; Orozco-Gutierrez, F.; Vega-Baudrit, J.; González-Paz, R.J. Thermal-Mechanical Characterization of Polyurethane Rigid Foams: Effect of Modifying Bio-Polyol Content in Isocyanate Prepolymers. *J. Renow. Mater.* **2017**, *5*, 220–230. [CrossRef]
41. Rangel-Vazquez, N.-A.; Sánchez-López, C. Spectroscopy Analyses of Polyurethane/Polyaniline IPN Using Computational Simulation (Amber, MM+ and PM3 Method). *Polímeros* **2014**, *24*, 1–11. [CrossRef]
42. Steinbach, J.C.; Schneider, M.; Hauler, O.; Lorenz, G.; Rebner, K.; Kandelbauer, A. A Process Analytical Concept for In-Line FTIR Monitoring of Polysiloxane Formation. *Polymers* **2022**, *12*, 2473. [CrossRef] [PubMed]

Disclaimer/Publisher's Note: The statements, opinions and data contained in all publications are solely those of the individual author(s) and contributor(s) and not of MDPI and/or the editor(s). MDPI and/or the editor(s) disclaim responsibility for any injury to people or property resulting from any ideas, methods, instructions or products referred to in the content.